

Perturbed Chain-Statistical Associating Fluid Theory Extended to Dipolar and Quadrupolar Molecular Fluids

Eirini K. Karakatsani and Ioannis G. Economou*

Molecular Thermodynamics and Modeling of Materials Laboratory, Institute of Physical Chemistry, National Center for Scientific Research "Demokritos", GR-15310 Aghia Paraskevi Attikis, Greece

Received: November 30, 2005; In Final Form: March 23, 2006

The perturbed chain statistical associating fluid theory (PC-SAFT) is extended to polar molecular fluids, namely dipolar and quadrupolar fluids. The extension is based on the perturbation theory for polar fluids by Stell and co-workers. Appropriate expressions are proposed for dipole–dipole, quadrupole–quadrupole, and dipole–quadrupole interactions. Furthermore, induced dipole interactions are calculated explicitly in the model. The new polar PC-SAFT model is relatively complex; for this purpose, a truncated polar PC-SAFT model is proposed using only the leading term in the polynomial expansion for polar interactions. The new model is used for the calculation of thermodynamic properties of various quadrupolar pure fluids. In all cases, the agreement between experimental data and model predictions is very good.

Introduction

Polar forces affect significantly the thermodynamic properties and phase equilibria of pure fluids and mixtures. Such fluids are often encountered in the chemical process industry, and explicit representation of polar forces in a thermodynamic model is necessary for the design and optimization of the relevant processes.¹ An elegant and still accurate treatment of polar forces is based on perturbation theory.² Short-range repulsive forces play a dominant role in the structure of a fluid and dispersion forces, polar forces, hydrogen bonding, and electrostatic forces can be considered as higher-order perturbations.

A number of theoretical models have been proposed over the last three decades for polar fluids based on perturbation theory.^{3–12} Larsen et al.³ proposed a simple Padé approximant to calculate polar interactions in spherical fluids by using the second- and third-order perturbation terms accounting combined for two-body and three-body contributions. Gubbins and Twu⁴ further extended the theory to polyatomic fluids, and Vimalchand and Donohue⁵ incorporated this theory into the perturbed anisotropic chain theory.

A major difference between the Larsen et al. theory and the Gubbins and Twu theory concerns the reference system considered. The former theory uses a simple hard-sphere reference fluid carrying central point multipoles, while the latter uses the (12, 6) Lennard–Jones reference fluid. A direct consequence of this difference is the approximation of double and triple integrals over pair and triple distribution functions by functions of reduced density only (in the Larsen et al. approach) and of both reduced density and temperature (in the Gubbins and Twu approach).^{3,4}

A quite different approach was proposed by Fischer and co-workers, who calculated the contributions of dipole–dipole and quadrupole–quadrupole interactions to the total Helmholtz free energy of the fluid by using extensive molecular dynamics (MD) simulation results.⁶ The new polar terms were incorporated in

the so-called BACKONE equation of state (EoS).^{7,8} BACKONE is an accurate EoS for both pure fluids and mixtures. When applied to mixtures of both dipolar and quadrupolar fluids, the model accounts for cross contributions by using effective dipole and quadrupole moments that are higher than experimental values.⁹

Benavides et al. have used a Padé approximant for quadrupole–quadrupole interactions together with a square-well EoS.¹⁰ The resulting quadrupolar square-well theoretical EoS (QSWTEOS) provided accurate prediction of the vapor–liquid saturation curve for nitrogen and carbon dioxide over a wide temperature range. However, for both fluids, the model over-predicted the critical point significantly. In the same spirit, a dipolar square-well theoretical EoS (DSWTEOS) and a unique octopolar square-well theoretical EoS (OSWTEOS) were proposed.^{11,12} Hydrogen bonding exhibited by water and ammonia molecules was accounted implicitly in DSWTEOS by using increased values for the dipolar moments of the two fluids compared to the experimental values (by 13 and 26%, respectively). A similar increase in the dipole moment of methanol was assumed by Twu and Gubbins when modeling the liquid–liquid immiscibility of the methanol/carbon dioxide/ethane mixture justified by the neglect of higher-order electrostatic terms in methanol.⁴

A powerful perturbation theory for associating fluids was proposed by Wertheim in the early 1990s based on a resummation expansion of the Helmholtz free energy.^{13,14} Wertheim's first-order thermodynamic perturbation theory (TPT-1) formed the basis for the statistical associating fluid theory (SAFT) and its subsequent modifications (most notably the perturbed chain-SAFT or PC-SAFT) that attracted substantial attention for pure fluid and mixture-phase equilibria calculations.^{15–17} In its original formulation, TPT-1 (and consequently SAFT) did not account explicitly for polar forces in order to avoid substantial increase of model complexity.¹⁴ An attempt to do so was proposed by Jog and Chapman, who developed expressions for dipole–dipole and quadrupole–quadrupole interactions based on molecular simulation results and by introducing a new adjustable parameter, which is the fraction of dipolar segments

* To whom all correspondence should be addressed. E-mail: economou@chem.demokritos.gr. Telephone: ++ 30 210 6503963. fax: ++ 30 210 6511766.

per chain, x^{DD} , and the fraction of quadrupolar segments per chain, x^{QQ} , respectively.¹⁸ These expressions were applied successfully to several pure polar substances and binary polar mixtures by Chapman and co-workers and Sadowski and co-workers.^{19–23} Independently, Gross proposed an extension of PC-SAFT to quadrupolar and dipolar fluids based on molecular simulation results for model polar fluids.^{24–25}

Recently,²⁶ SAFT and PC-SAFT were extended to dipolar fluids by using a simple but still accurate perturbation term based on the Stell and co-workers model for polar spherical fluids.³ The new models were shown to be accurate for both pure and mixture dipolar fluids. In this work, PC-SAFT is further extended to account explicitly for higher-order quadrupole–quadrupole, dipole–quadrupole, as well as dipole–induced dipole interactions, based again on the model of Stell and co-workers.³ The methodology presented here for PC-SAFT can be applied also to SAFT. Two different approaches are elucidated: in the first case, the exact second- and third-order perturbation terms of Stell and co-workers are used, while in the second case a simplified version of the two terms is used. Consequently, we will refer to these models as PC-polar SAFT (PC-PSAFT) and truncated PC-PSAFT (tPC-PSAFT). In the case of tPC-PSAFT, an additional pure component parameter is introduced that accounts for the simplification of the polar term of the model.

Both Jog and Chapman polar SAFT¹⁸ and PC-PSAFT presented here are segment-based models. In polar SAFT, multipoles are assumed to be located on certain segments of a chain molecule, while in our case, multipoles are assumed to be uniformly distributed over all segments, i.e., each segment possesses an average dipole or quadrupole moment of magnitude μ/m or Q/m , respectively. The segmental approach is important when it comes to mixtures of large molecules because it is known to give better representation than using mole-fraction-averaged interactions between molecular dipoles or quadrupoles.⁵

Model Development

In PC-SAFT, the reference fluid is the hard-chain fluid, and perturbation accounts for weak dispersion interactions and association. Additional terms in the perturbation expansion are added here to account for polar and induced polar interactions. Consequently, the residual Helmholtz free energy per mole for PC-PSAFT is expressed as:

$$\begin{aligned} \frac{a^{\text{res}}(T, \rho)}{RT} &= \frac{a(T, \rho)}{RT} - \frac{a^{\text{ideal}}(T, \rho)}{RT} \\ &= \frac{a^{\text{ref}}(T, \rho)}{RT} + \frac{a^{\text{disp}}(T, \rho)}{RT} + \frac{a^{\text{polar}}(T, \rho)}{RT} + \frac{a^{\text{ind}}(T, \rho)}{RT} \\ &= \frac{a^{\text{hs}}(T, \rho)}{RT} + \frac{a^{\text{chain}}(T, \rho)}{RT} + \frac{a^{\text{assoc}}(T, \rho)}{RT} + \\ &\quad \frac{a^{\text{disp}}(T, \rho)}{RT} + \frac{a^{\text{polar}}(T, \rho)}{RT} + \frac{a^{\text{ind}}(T, \rho)}{RT} \quad (1) \end{aligned}$$

where T and ρ are the temperature and density of the system, respectively, and the residual Helmholtz free energy is calculated with respect to the Helmholtz free energy for the ideal gas at the same T and ρ .

For the hard-sphere term of eq 1, the Carnahan–Starling expression is used, so that:

$$\frac{a^{\text{hs}}}{RT} = m \frac{4\eta - 3\eta^2}{(1 - \eta)^2} \quad (2)$$

where m is the number of spherical segments per molecule, and η is the reduced density evaluated from the expression:

$$\eta = \tau \rho m v^o \quad (3)$$

where $\tau = 0.74048$, v^o is the close-packed hard-core volume of the fluid, which is calculated from the temperature-independent soft-core volume of the fluid, according to the following expression:

$$v^o = v^{\text{oo}}(1 - 0.12 \exp(-3u/kT))^3 \quad (4)$$

where u/k is a dispersion energy per segment parameter. m , v^{oo} (alternatively the segment diameter, σ , calculated from the expression $\sigma = (6\tau v^{\text{oo}}/\pi N_{\text{Av}})^{1/3}$ can be used), and u/k are the three characteristic nonassociating parameters for pure fluids.

For the chain term, the following expression is used based on Wertheim TPT-1:¹⁵

$$\frac{a^{\text{chain}}}{RT} = (1 - m) \ln \frac{1 - 0.5\eta}{(1 - \eta)^3} \quad (5)$$

and for association, the Helmholtz free energy is calculated from the expression:¹⁵

$$\frac{a^{\text{assoc}}}{RT} = \sum_{A=1}^M \left[\ln X^A - \frac{X^A}{2} \right] + 0.5M \quad (6)$$

where M is the number of association sites per molecule, and X^A is the mole fraction of molecules not bonded at site A. In eq 6, the sum is taken over all association sites of the molecule. The quantity X^A is calculated from the expression:¹⁵

$$X^A = (1 + \sum_{B=1}^M \rho X^B \Delta^{\text{AB}})^{-1} \quad (7)$$

where Δ^{AB} is the association strength evaluated from the following expression:¹⁵

$$\Delta^{\text{AB}} = \sqrt{2} v^{\text{oo}} \frac{1 - 0.5\eta}{(1 - \eta)^3} [\exp(\epsilon^{\text{AB}}/kT) - 1] \kappa^{\text{AB}} \quad (8)$$

In eq 8, the two pure component parameters for association are introduced: the energy of association, ϵ^{AB}/k , and the volume of association, κ^{AB} .

In PC-SAFT, the dispersion contribution to the Helmholtz free energy is given by:¹⁷

$$\frac{a^{\text{disp}}}{RT} = -2\pi\rho I_1(\eta, m) m^2 \frac{1}{T} \sigma^3 - \pi\rho m C_1 I_2(\eta, m) m^2 \left(\frac{1}{T}\right)^2 \sigma^3 \quad (9)$$

where $\tilde{T} = T/(u/k)$ and C_1 is the following compressibility expression:

$$\begin{aligned} C_1 &= \left(1 + m \frac{8\eta - 2\eta^2}{(1 - \eta)^4} + \right. \\ &\quad \left. (1 - m) \frac{20\eta - 27\eta^2 + 12\eta^3 - 2\eta^4}{[(1 - \eta)(2 - \eta)]^2} \right)^{-1} \quad (10) \end{aligned}$$

The integrals in the perturbation theory are evaluated from the following series expansions:¹⁷

$$I_1(\eta, m) = \sum_{i=0}^6 a_i(m) \eta^i \quad (11)$$

$$I_2(\eta, m) = \sum_{i=0}^6 b_i(m) \eta^i \quad (12)$$

where the coefficients α_i and b_i are functions of the chain length:

$$a_i(m) = a_{0i} + \frac{m-1}{m} a_{1i} + \frac{m-1}{m} \frac{m-2}{m} a_{2i} \quad (13)$$

$$b_i(m) = b_{0i} + \frac{m-1}{m} b_{1i} + \frac{m-1}{m} \frac{m-2}{m} b_{2i} \quad (14)$$

The coefficients α_{ji} and b_{ji} are given by Gross and Sadowski¹⁷ and are not repeated here.

For polar and induced polar interactions, the pioneering work of Stell and co-workers is used³. More specifically, dipole–dipole, quadrupole–quadrupole, and dipole–quadrupole interactions are calculated by using a simple but accurate Padé approximant:

$$\frac{a^{\text{polar}}}{RT} = m \frac{a_2^{\text{polar}}}{1 - a_3^{\text{polar}}/a_2^{\text{polar}}} \quad (15)$$

where a_2^{polar} and a_3^{polar} are the second- and third-order perturbation terms. The third-order perturbation term accounts for two-body and three-body contributions because it has been shown that three-body contributions are significant for the Helmholtz free energy and cannot be neglected.^{27,28} Consequently:

$$\frac{a_3^{\text{polar}}}{RT} = \frac{a_{3,2}^{\text{polar}}}{RT} + \frac{a_{3,3}^{\text{polar}}}{RT} \quad (16)$$

The induced polar term is based on a Padé approximant similar to the one for permanent polar interactions:

$$\frac{a^{\text{ind}}}{RT} = m \frac{a_2^{\text{ind}}}{1 - a_3^{\text{ind}}/a_2^{\text{ind}}} \quad (17)$$

where a_2^{ind} and a_3^{ind} are the second- and third-order perturbation terms, respectively. It should be mentioned here that pair additivity does not apply for induction electrostatic interactions as it is for the other electrostatic interactions. Consequently, the perturbation expansion around the pair potential of induced dipoles may not be that accurate.²⁹

The first-order perturbation terms for polar and induced polar interactions, that are a_1^{polar} and a_1^{ind} , respectively, are exactly zero for spherical molecules and nonzero but small for hard dumbbell and hard spherocylinder fluids, as shown by Vega.³⁰ The analytical calculation of specific molecular anisotropies is beyond the purpose of this work. Consequently, for all fluids examined here, it is assumed that: $a_1^{\text{polar}} = a_1^{\text{ind}} = 0$.

Larsen et al.³ proposed accurate expressions for the perturbation terms of eqs 15–17 for spherical fluids. Here, these expressions are applied to nonspherical associating fluids so that:

$$\frac{a_2^{\text{polar}}}{RT} = -\frac{\rho^*}{\tilde{\tau}^2} \left[\frac{\tilde{\mu}^4}{6} I_6^{\text{ref}}(\rho^*) + \frac{\tilde{\mu}^2 \tilde{Q}^2}{2} I_8^{\text{ref}}(\rho^*) + \frac{7\tilde{Q}^4}{10} I_{10}^{\text{ref}}(\rho^*) \right] \quad (18)$$

$$\frac{a_{3,2}^{\text{polar}}}{RT} = \frac{\rho^*}{\tilde{\tau}^3} \left[\frac{2}{5} \tilde{\mu}^4 \tilde{Q}^2 I_{11}^{\text{ref}}(\rho^*) + \frac{12}{35} \tilde{\mu}^2 \tilde{Q}^4 I_{13}^{\text{ref}}(\rho^*) + \frac{36}{245} \tilde{Q}^6 I_{15}^{\text{ref}}(\rho^*) \right] \quad (19)$$

$$\frac{a_{3,3}^{\text{polar}}}{RT} = \frac{(\rho^*)^2}{\tilde{\tau}^3} \left[\frac{\tilde{\mu}^6}{54} I_{\text{TD}}^{\text{ref}}(\rho^*) + \frac{\tilde{\mu}^4 \tilde{Q}^2}{480} I_{\text{DDQ}}^{\text{ref}}(\rho^*) + \frac{\tilde{\mu}^2 \tilde{Q}^4}{640} I_{\text{DQQ}}^{\text{ref}}(\rho^*) + \frac{\tilde{Q}^6}{6400} I_{\text{TQ}}^{\text{ref}}(\rho^*) \right] \quad (20)$$

and:

$$\frac{a_2^{\text{ind}}}{RT} = -\frac{\rho^*}{\tilde{\tau}} \tilde{\mu}^2 \tilde{\alpha} I_6^{\text{ref}}(\rho^*) \quad (21)$$

$$\frac{a_3^{\text{ind}}}{RT} = \frac{a_{3,12}^{\text{ind}}}{RT} + \frac{a_{3,21}^{\text{ind}}}{RT} \approx \frac{a_{3,12}^{\text{ind}}}{RT} = \frac{1}{6} \left(\frac{\rho^*}{\tilde{\tau}} \right)^2 \tilde{\mu}^4 \tilde{\alpha} I_{\text{TD}}^{\text{ref}}(\rho^*) \quad (22)$$

where: ref stands for the reference fluid, that is, the hard-sphere fluid for Larsen et al. and the associating hard-chain fluid here,

$$\tilde{\mu} = 85.12 \frac{\mu/m}{\sqrt{(u/k)\sigma^3}}, \quad \tilde{Q} = 85.12 \frac{Q/m}{\sqrt{(u/k)\sigma^5}},$$

$$\tilde{\alpha} = \frac{\alpha}{m\sigma^3} \quad \text{and} \quad \rho^* = \rho\sigma^3$$

In these expressions, μ is the dipole moment of the fluid (in D), Q is its quadrupole moment (in DÅ) and α is its polarizability (in Å³). In eq 22, the second term in the three-body term is very small and is ignored.

A practical issue here is the choice of the value that should be used for multipole moments and the polarizability. For dipole moments, Vega et al. showed that the orientation of the dipole has a considerable effect on the thermodynamic and structural properties of the fluid.³¹ On the other hand, the experimental determination of quadrupole moment of a fluid is rather difficult. Considerable differences in the quadrupole moment values of a given fluid can be found from different sources. According to Stogryn and Stogryn,³² the two most reliable experimental methods for determining quadrupole moments are based on the induced birefringence developed by Buckingham and co-workers³³ and on the measurement of anisotropy in diamagnetic susceptibility by molecular beam resonance methods proposed by Ramsey and co-workers³⁴ and by Gräff and co-workers.³⁵ Still, for many quadrupolar molecules, no such experiments have been carried out.

For molecular fluids, polarizability is a tensor, but for spherically symmetric charge distributions, it is reduced to a scalar quantity and average polarizability values are usually adequate for physical property calculations.³⁶ In general, the molecular dipole moment (value in vacuo) and the isotropic mean polarizability values are known accurately for many substances and have been determined experimentally and/or through quantum chemical calculations.³⁶

In the model proposed here, segmental polar parameters $\tilde{\mu}$ and \tilde{Q} are calculated by assuming that dipole and quadrupole moments are evenly distributed over the entire molecule. An alternative approach proposed by Sauer and Chapman²⁰ is to calculate the polar segment fraction of the molecule. In this approach, however, an additional adjustable parameter is introduced. The two-body and three-body integrals in eqs 18–22 are further analyzed below.

In eqs 18–22, a number of double and triple integrals appear that are of the form:

$$I_n^{\text{ref}}(\rho^*) \equiv 4\pi \int_0^\infty g^{\text{ref}}(\rho^*, y) y^{2-n} dy$$

$$n = 6, 8, 10, 11, 13, 15 \quad (23)$$

$$I_{\text{triple}}^{\text{ref}}(\rho^*) \equiv \int g_{123}^{\text{ref}}(R, s, z) W_{\text{triple}}(R, s, z) d\vec{s} d\vec{z} \quad (24)$$

triple = TD, DDQ, DQQ, TQ

where $y = r/\sigma$, and $\vec{R} = \vec{r}_{12}/\sigma$, $\vec{s} = \vec{r}_{13}/\sigma$, $\vec{z} = \vec{r}_{23}/\sigma$ are reduced radii between bodies 1, 2, and 3, $g^{\text{ref}}(\rho^*, y)$ and $g_{123}^{\text{ref}}(R, s, z)$ are the hard-sphere pair and triple radial distribution functions, and W_{triple} are the individual angularly averaged three-body potentials, represented collectively. Thanks to the remarkable smoothness of the above double and triple integrals as functions of ρ^* , Larsen et al. approximated them by simple density polynomials of fifth- and third-order, respectively, that are used also here for the case of associating hard-chain reference fluid:

$$I_n^{\text{ref}} = \sum_{i=0}^5 J_{i,n}^{\text{double}}(\rho^*)^i \quad (25)$$

$$I_{\text{triple}}^{\text{ref}} = \sum_{i=0}^3 J_{i,n}^{\text{triple}}(\rho^*)^i \quad (26)$$

resulting in the formulation of simple analytic expressions³. Coefficients $J_{i,n}^{\text{double}}$ and $J_{i,n}^{\text{triple}}$ are given in the original reference³ and are not repeated here.

With a noncubic EoS, most of the computing time is spent in calculating summations and not density.³⁷ In addition, because there is no perturbation theory for both single- and cross-multipolar contributions, application of Wertheim's solution of the mean-spherical approximation (MSA)³⁸ for the spherical segments of the chainlike molecules, incorporation of the chain-length dependence of molecular fluids, and finally, extension of the model to real molecules is a reasonable approach to tackle such a complex problem.

The major objective here is not to optimize the SAFT EoS family, but rather to develop a simple meaningful basis for describing polar substances and mixtures. For this reason, a simpler model for polar fluids is further developed, suitable for engineering calculations. The basic idea behind this simpler perturbation model is based on the following arguments. At short separations, all molecules are subject to strong repulsive interactions (excluded-volume effects). If they hydrogen bond, they are subject to strong attractive interactions, restricted also to a narrow range of angles formed between the atoms involved.^{39,40} As far as long-range interactions are concerned, with the exception of some isotropic interactions of the Lennard–Jones type that are present at any distance preventing collapse of the system, electrostatic interactions are gradually “turned on” outside the range of the hydrogen-bond interaction for associating fluids and, in any case, beyond the first coordination shell.³⁹ This has been confirmed by several Monte Carlo (MC) and MD simulation results.³⁹

MC simulations using realistic force fields for aqueous mixtures have been used to quantify the accessible volume to solute molecules. It was shown that the accessible volume to nonpolar solutes is considerably smaller compared to the accessible volume to polar molecules of the same Lennard–Jones diameter. Consequently, setting the hard-core diameter of a polar solute molecule in water equal to its Lennard–Jones diameter is highly unphysical.⁴¹ Therefore, it is reasonable to attribute greater importance to the range of polar interactions instead of their strength and to specify a segment diameter, σ_p , beyond which long-range electrostatic interactions dominate. Such decomposition is the basis for the development of simple and more accurate EoS for polar fluids.

One way of determining such an effective polar radius is based on the deviations of functions that describe local fluid structure (i.e., the site–site functions, the dipole–dipole correlation function, and the full pair correlation function) for systems of different short ranges compared to the full long-range system.⁴² Such studies allow determination of the switching range (from short- to long-range interactions). Results have been presented for water, methanol, acetone, and carbon dioxide. In the case of oxygen-containing associating molecules, the first peaks of g_{OO} and g_{OH} are taken approximately as the manifestation of the hydrogen bond structure.⁴³ In this work, the effective polar interactions segment diameter, σ_p , is used to characterize effective polar interactions and is treated as an adjustable parameter.

As already mentioned, one of the goals of this work is to develop a relatively simple but still accurate model for engineering calculations. For this reason, a truncated PC-SAFT (tPC-PSAFT) is proposed by approximating the double and triple integrals in eqs 25 and 26 with their first terms that correspond to the 0th-order coefficients, $J_{0,n}^{\text{double}}$ and $J_{0,n}^{\text{triple}}$, respectively. These coefficients are given analytically from the expressions³:

$$J_{0,n}^{\text{double}} = \frac{4\pi}{n-3}, \quad n \geq 4 \quad (27)$$

$$J_{0,n}^{\text{triple}} = \begin{cases} \frac{5\pi^2}{3} & \text{for TD} \\ \frac{424\pi^2}{25} & \text{for DDQ and DQQ} \\ 54\pi^2 & \text{for TQ} \end{cases} \quad (28)$$

In this way, the polar terms in tPC-PSAFT simplify to the following expressions:

$$\frac{a_2^{\text{polar}}}{RT} = -\left(\frac{1}{T}\right)^2 \frac{\eta}{K^3} \left[\frac{4}{3} \tilde{\mu}^4 + \frac{12}{5} \frac{\tilde{\mu}^2 \tilde{Q}^2}{K^2} + \frac{12}{5} \frac{\tilde{Q}^4}{K^4} \right] \quad (29)$$

$$\frac{a_{3,2}^{\text{polar}}}{RT} = \left(\frac{1}{T}\right)^3 \frac{\eta}{K^8} \left[\frac{6}{5} \tilde{\mu}^4 \tilde{Q}^2 + \frac{144}{175} \frac{\tilde{\mu}^2 \tilde{Q}^4}{K^2} + \frac{72}{245} \frac{\tilde{Q}^6}{K^4} \right] \quad (30)$$

$$\frac{a_{3,3}^{\text{polar}}}{RT} = \left(\frac{1}{T}\right)^3 \frac{\eta^2}{K^3} \left[\frac{10}{9} \tilde{\mu}^6 + \frac{159}{125} \frac{\tilde{\mu}^4 \tilde{Q}^2}{K^2} + \frac{689}{1000} \frac{\tilde{\mu}^2 \tilde{Q}^4}{K^4} + \frac{243}{800} \frac{\tilde{Q}^6}{K^6} \right] \quad (31)$$

where K is a dimensionless quantity that accounts for the spatial range of polar interactions compared to hard-sphere interactions, $K = \sigma_p/\sigma$. It is noted that the dipolar terms in the right-hand side of eqs 29 and 31 have been used successfully by Nezbeda and co-workers^{44,45} and by us²⁶ for dipolar pure fluids and mixtures.

In a similar way, simplified expressions are proposed for the dipole–induced dipole two-body and three-body terms:

$$\frac{a_2^{\text{ind}}}{RT} = -\frac{8}{T} \frac{\eta}{K^3} \tilde{\mu}^2 \tilde{a} \quad (32)$$

$$\frac{a_3^{\text{ind}}}{RT} = 10 \left(\frac{1}{T}\right)^2 \frac{\eta^2}{K^3} \tilde{\mu}^4 \tilde{a} \quad (33)$$

Most engineering models for polar fluids ignore the cross dipole–quadrupole terms, and so these models become less accurate when applied to mixtures with both dipolar and quadrupolar components. In the case where components have

TABLE 1: Pure-Component Parameters for PC-PSAFT Equation of State for Quadrupolar Fluids

	m [—]	ν^{oo} [mL/mol]	u/k [K]	Q [DÅ]	T [K]	% AAD ^a	
						P^{sat}	ρ^{liq}
nitrogen	1.140	16.9	110.10	1.36 ^b	82–126	1.16	2.81
carbon dioxide	2.042	9.5	154.01	4.3 ^c	217–301	0.85	0.93
oxygen	1.087	14.5	117.23	0.39 ^b	65–153	1.29	1.06
ethylene	1.546	17.4	180.06	1.50 ^b	125–280	0.29	0.50
acetylene	2.203	10.3	164.18	3.00 ^b	212–305	0.78	0.82
propadiene	1.402	24.7	267.08	4.37	208–389	1.45	2.12
benzene	2.345	21.9	290.11	8.50 ^c	334–557	0.57	0.71
toluene	2.807	22.0	284.65	7.92 ^c	286–586	0.92	0.96
ethylbenzene	3.056	23.5	287.65	7.92	214–611	0.50	1.16
propylbenzene	3.338	24.9	289.92	7.92	221–632	1.50	1.74
<i>p</i> -xylene	3.216	22.5	281.29	7.69 ^c	344–610	0.92	1.27
naphthalene	2.902	26.9	355.30	13.70 ^d	424–741	0.47	1.65
methylnaphthalene	3.360	25.8	344.92	13.70	291–764	2.41	1.33
ethylnaphthalene	3.715	25.7	335.40	13.70	311–768	2.08	1.13
acetonitrile	2.556	12.9	295.50	1.8	353–518	1.43	4.68
water	1.749	6.6	169.53	2.69 ^c	278–638	0.55	1.17
average						1.07	1.50

^a % AAD = percentage average absolute deviation. For water, $\epsilon^{\text{hb}}/k = 1131.0$ K, $\kappa^{\text{hb}} = 0.2001$, $\mu = 1.85$ D, and $\alpha = 1.49$ Å³. Ethylbenzene and propylbenzene quadrupole moments were set equal to toluene quadrupole moment. Methylnaphthalene and ethylnaphthalene quadrupole moments were set equal to naphthalene quadrupole moment. ^b Stogryn, D. E.; Stogryn, A. D. *Mol. Phys.* **1966**, *11*, 371. ^c Reynolds, L.; Gardecki, J. A.; Frankland, S. J. V.; Horng, M. L.; Maroncelli, M. *J. Phys. Chem.* **1996**, *100*, 10337. ^d Calvert, R. L.; Ritchie, G. L. D. *J. Chem. Soc., Faraday Trans.* **1980**, *76*, 1249.

large differences in their polar moments, a temperature-dependent mixture parameter is used, as for example in BACKONE EoS.⁹

A limitation of the tPC-PSAFT model is that, by applying MSA to the chain segments, the full expressions are replaced by their low-density limits. The incorporation of an adjustable parameter to the model is believed to overcome up to a certain degree this weakness of the theory. The assumption of temperature-independent double and triple integrals is also a crude approximation made in both PC-PSAFT and tPC-PSAFT, valid only for molecules with hard repulsive interactions.

Results and Discussion

In this work, PC-PSAFT and tPC-PSAFT models were applied to real polar fluids. The earlier work of Karakatsani et al.²⁶ focused on dipolar fluids. Consequently, here, the focus is on quadrupolar fluids. Very accurate correlations developed by DIPPR⁴⁶ were used as pseudo-experimental data for the regression of model pure component parameters. PC-PSAFT nonassociating parameters (m , u/k , and ν^{oo}) and tPC-PSAFT nonassociating parameters (m , u/k , ν^{oo} , and ν^{p}) were fitted to experimental vapor pressure and saturated liquid density data over a wide temperature range, up to very close to the critical point ($0.99 T_c$). Multiple moments and polarizability were taken equal to the experimental values without any further adjustment.

In Tables 1 and 2, the pure component parameters for PC-PSAFT and tPC-PSAFT, the temperature range used for parameter regression and the average absolute deviation between experiments and model calculations are shown for 16 different quadrupolar fluids. For multiparameter models, it is often the case that more than one set of parameters provide good correlation of thermodynamic properties. In many cases though, one or more of the parameter values are highly unrealistic. Furthermore, in models with a strong theoretical basis whose parameters have a clear physical meaning, it is expected that parameter values vary in a systematic way with molecular weight (MW) for a homologous series of components. In Figure 1, the variation of m , $m\nu^{\text{oo}}$, and u/k with MW for benzene derivatives and naphthalene derivatives for PC-PSAFT is shown. Very similar results are obtained for the case of tPC-PSAFT. In all cases, m and $m\nu^{\text{oo}}$ vary linearly with MW, while u/k assumes a relatively constant value. Consequently, these parameters can be safely extrapolated to components of higher MW.

Experimental data and model correlations are shown graphically in Figure 2 for the vapor pressure and in Figure 3 for the saturated liquid density of various components. Interestingly, the overall accuracy of the two models is similar. One may conclude that the loss of accuracy in the polar terms due to the model simplification in tPC-PSAFT is recovered by the addition of the extra parameter, ν^{p} . In Figure 4, the percentage deviation between experimental data and calculations from the two models

TABLE 2: Pure-Component Parameters for TPC-PCSAFT Equation of State for Quadrupolar Fluids

	m [—]	ν^{oo} [mL/mol]	u/k [K]	Q [DÅ]	ν^{p} [mL/mol]	T [K]	% AAD ^a	
							P^{sat}	ρ^{liq}
nitrogen	1.010	19.3	122.01	1.36 ^b	37.3	82–126	2.13	1.69
carbon dioxide	1.912	9.9	157.97	4.3 ^c	11.2	217–301	0.42	0.49
oxygen	1.113	14.1	115.81	0.39 ^b	33.1	65–153	1.04	1.40
ethylene	1.553	17.3	179.74	1.50 ^b	38.4	125–280	0.31	0.50
acetylene	2.296	9.8	162.72	3.00 ^b	37.7	212–305	0.77	0.71
propadiene	1.857	18.0	231.62	13.7	25.7	208–389	1.40	1.92
benzene	2.428	21.0	288.17	8.50 ^c	43.7	334–557	0.50	0.60
toluene	2.811	21.9	285.39	7.92 ^c	44.6	286–586	0.60	0.96
ethylbenzene	3.086	23.2	286.79	7.92	77.1	214–611	0.45	1.12
propylbenzene	3.337	24.8	287.57	7.92	299.1	221–632	1.19	1.68
<i>p</i> -xylene	3.219	22.5	281.72	7.69 ^c	110.7	344–610	0.76	1.27
naphthalene	2.858	27.3	353.71	13.70 ^d	27.9	424–741	0.92	1.48
methylnaphthalene	3.438	25.1	343.26	13.70	215.5	291–764	2.14	1.22
ethylnaphthalene	3.623	26.4	337.43	13.70	27.2	311–768	1.80	1.18
acetonitrile	2.561	12.9	295.20	1.8	71.7	353–518	1.44	4.67
water	1.600	7.4	58.06	2.69	7.7	278–641	0.98	2.24
average							1.05	1.45

^a % AAD = percentage average absolute deviation. For water, $\epsilon^{\text{hb}}/k = 1639.5$ K, $\kappa^{\text{hb}} = 0.1812$, $\mu = 1.85$ D, and $\alpha = 1.49$ Å³. Ethylbenzene and propylbenzene quadrupole moments were set equal to toluene quadrupole moment. Methylnaphthalene and ethylnaphthalene quadrupole moments were set equal to naphthalene quadrupole moment. ^b Stogryn, D. E.; Stogryn, A. D. *Mol. Phys.* **1966**, *11*, 371. ^c Reynolds, L.; Gardecki, J. A.; Frankland, S. J. V.; Horng, M. L.; Maroncelli, M. *J. Phys. Chem.* **1996**, *100*, 10337. ^d Calvert, R. L.; Ritchie, G. L. D. *J. Chem. Soc., Faraday Trans.* **1980**, *76*, 1249.

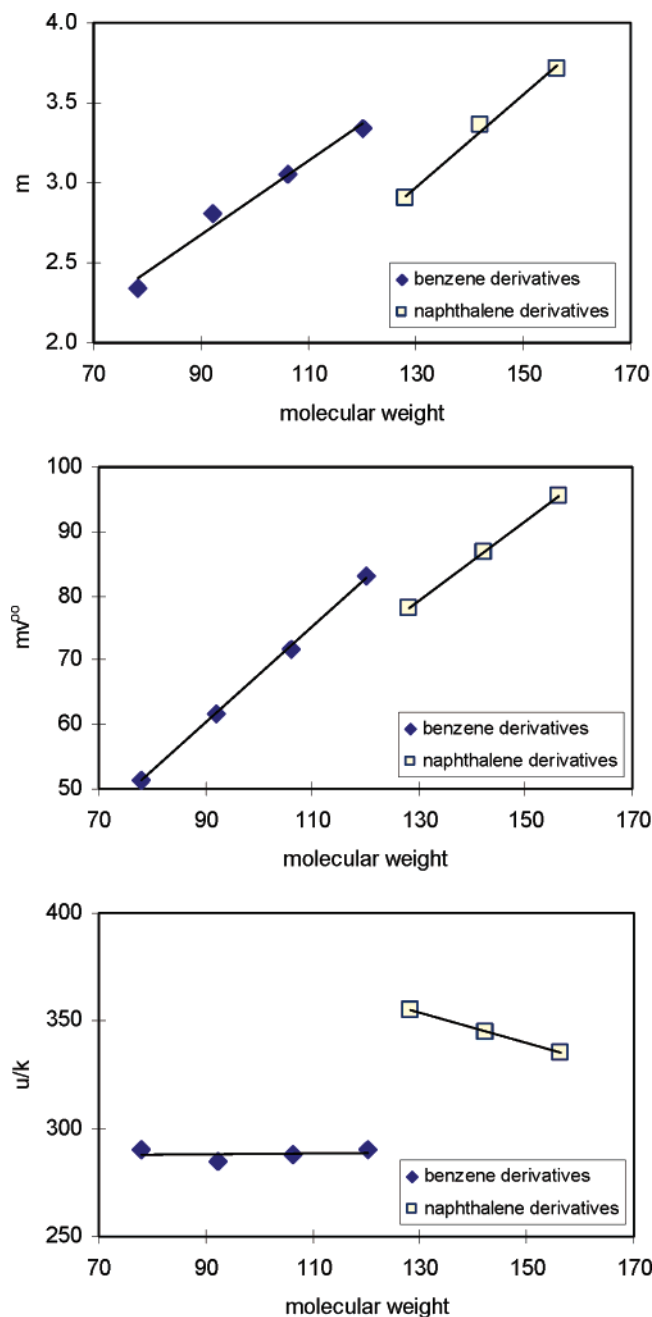


Figure 1. PC-SAFT parameters for benzene derivatives and naphthalene derivatives: (a) m , (b) mv^{po} , and (c) u/k .

is shown over the entire temperature range examined for (a) the vapor pressure and (b) the saturated liquid density of two representative quadrupolar fluids, that is, carbon dioxide and ethylene. For the case of carbon dioxide, tPC-SAFT is more accurate than PC-SAFT, while for ethylene, the two models are of similar accuracy. These results can be compared also with other model predictions from the literature. For example, comparison against BACKONE calculations⁷ reveals that the models presented here are of the same accuracy as this other model.

The accuracy of the new models for carbon dioxide and nitrogen are further examined at compressed liquid and supercritical conditions. Both fluids are used widely for high-pressure applications, and the accurate description of their density and other properties over a wide range of conditions is very important. In Figure 5, a pressure vs density diagram for the two fluids is shown that includes the saturation curve, com-

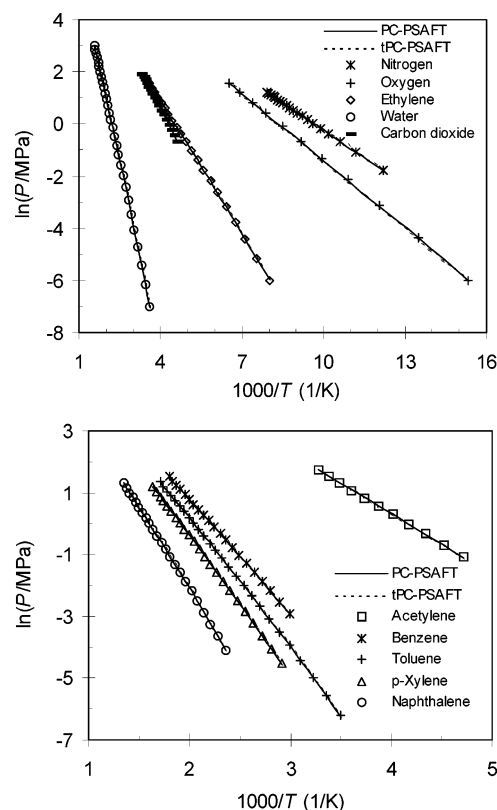


Figure 2. Experimental data (points) and EoS correlation (lines) for the vapor pressure of nitrogen, oxygen, ethylene, water, and carbon dioxide (top), and acetylene, benzene, toluene, *p*-xylene, and naphthalene (bottom).

pressed liquid, and supercritical fluid conditions. Both models are very accurate in all cases. Nitrogen is a low-quadrupole-moment fluid. However, quadrupole–quadrupole interactions are larger than dispersion interactions, and so polar interactions affect considerably the thermodynamic properties of this fluid.^{1,10}

Water is a unique complex fluid whose molecules interact through weak dispersion interactions, dipolar and quadrupolar interactions, and hydrogen-bonding interactions. Although it is the most common fluid on earth, there is still some lack of understanding of how the microscopic structure affects its thermodynamic properties. According to a relatively recent molecular simulation study by Nezbeda and Lísal⁴⁷ using the TIP4P force field, the long-range electrostatic forces contribute only marginally to the thermodynamic functions of water. Consequently, explicit account of polar interactions has a minor but still appreciable effect on the EoS properties. Nezbeda and Weingerl⁴⁵ provided a quantitative estimate of the improvement in pressure for model water and real water by accounting for polar interactions compared to the reference fluid, accounting for short-range interactions alone (repulsions and hydrogen bonding). As a result, it is expected that the models developed here will offer an improvement for water properties compared to original PC-SAFT.

The number of hydrogen-bonding sites per water molecule in a macroscopic model has been investigated extensively.^{16,48–50} The two-site model results in linear oligomers, while the three- and four-site models result in three-dimensional hydrogen-bonding clusters that are closer to reality.^{51,52} In this work, a four-site model was used for water assuming two electron donor sites (the two lone pairs of electrons on the oxygen atom) and two electron acceptor sites (the two hydrogen atoms). Furthermore, dipole–dipole, quadrupole–quadrupole, dipole–quad-

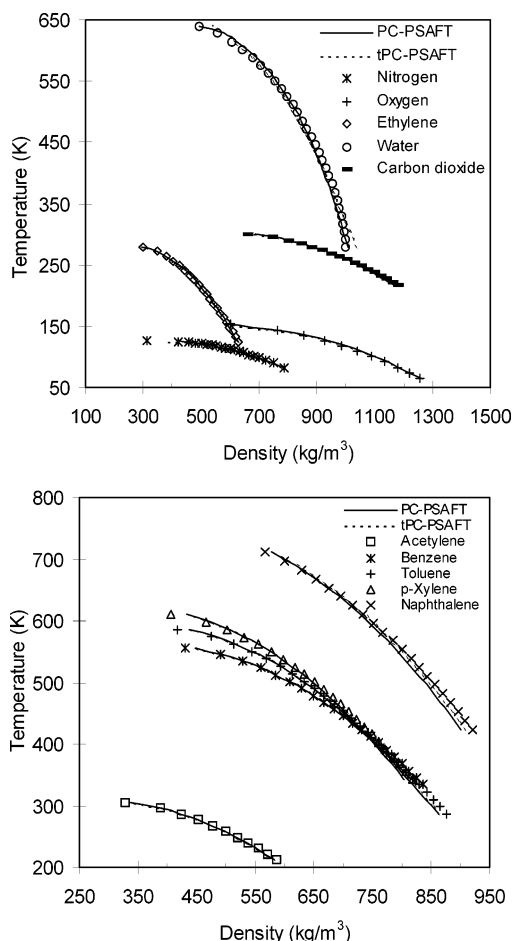


Figure 3. Experimental data (points) and EoS correlation (lines) for the saturated liquid density of nitrogen, oxygen, ethylene, water, and carbon dioxide (top), and acetylene, benzene, toluene, *p*-xylene, and naphthalene (bottom).

rupole, and dipole–induced dipole interactions were accounted explicitly. In Tables 1 and 2, the model parameters for PC-PSAFT and tPC-PSAFT are shown. The agreement between experimental data and model correlation is very good. In addition, the association energy parameter, ϵ^{hb}/k , for water compares very well with the experimental value for the enthalpy of hydrogen bonding. According to Luck,⁵³ $\Delta H/k = 1813$ K, while for PC-PSAFT, $\epsilon^{hb}/k = 1131.0$ K, and for tPC-PSAFT, $\epsilon^{hb}/k = 1639.5$ K.

A simple comparison of the relative magnitude of various types of intermolecular interactions, independently from the macroscopic model, can be based on the general potential energy expression:¹

$$\Gamma_{ii}(r) = -\frac{B}{r^6} \quad (34)$$

where Γ_{ii} is the potential energy between two identical molecules i at distance r . eq 34 can be used for dipole–dipole interactions, dipole–induced dipole interactions, and Lennard–Jones attractive interactions. For quadrupole–quadrupole interactions, the denominator is r^{10} . To develop a common basis for comparison, we evaluated Γ_{ii}^{qq} at distance $r = 2r_{vdW}$, where r_{vdW} is the water van der Waals radius, taken from the very accurate TIP4P force field for water⁵⁴ and the quantity $B^{QQ} = B/[(2r_{vdW})^4]$ was calculated. It turns out that:¹ $B^{DD} = 203$, $B^{D-indD} = 10.8$, $B^{LJ} = 38.1$, and $B^{QQ} = 4.6$ (all in 10^{-79} J/m⁶) at 0 °C.

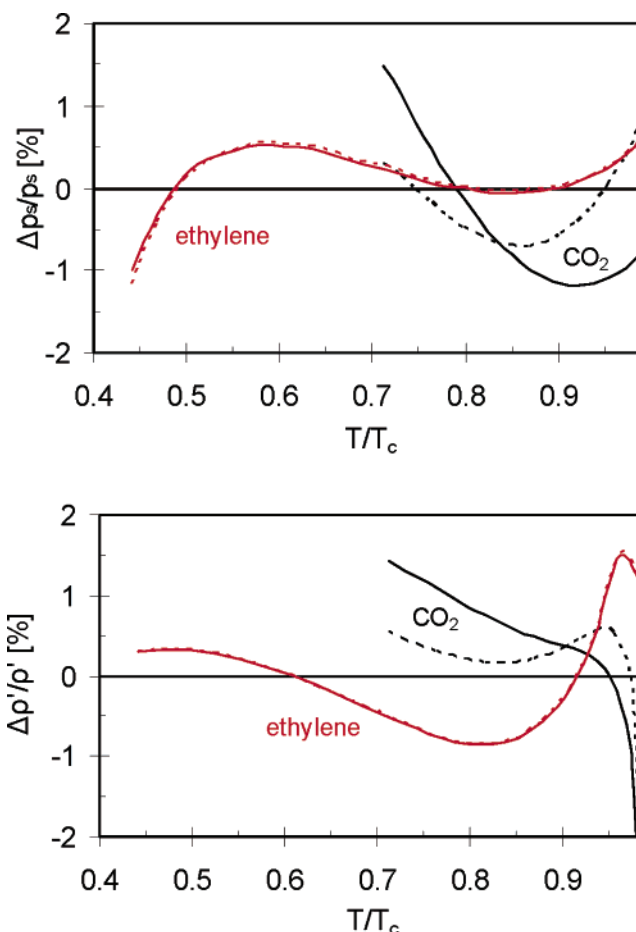


Figure 4. Percentage deviation between experimental data and model calculations for (a) vapor pressure and (b) saturated liquid density for carbon dioxide and ethylene obtained from PC-PSAFT (solid lines) and tPC-PSAFT (dotted lines).

An alternative way to evaluate the relative contribution of the various terms is presented in Figure 6. The relative contributions in pressure and in chemical potential are shown for the case of saturated liquid water at 460 K. Interestingly, the dispersion interactions and hydrogen bonding are similar and dominate both property values, while hard-chain and polar contributions are lower. Finally, the induced polar term is very small, in these conditions.

An important thermodynamic fluid property is the second virial coefficient, B , which can be calculated from the expression (this B is different than B in the numerator of eq 34):

$$B = \frac{1}{2RT} \left. \frac{\partial^2 P}{\partial \rho^2} \right|_{\rho=0} \quad (35)$$

For an EoS tuned mostly to saturated properties, prediction of B that accounts for low-density two-body interactions is a critical test.

In eq 35, the contribution due to polar interactions is:

$$B^{\text{polar}} = \frac{m(a_2^{\text{polar}} - a_{3,2}^{\text{polar}})}{\rho(1 - a_{3,2}^{\text{polar}}/a_2^{\text{polar}})^2} \quad (36)$$

and the contribution due to induced polar interactions is:

$$B^{\text{ind}} = m \frac{a_2^{\text{ind}}}{\rho} \quad (37)$$

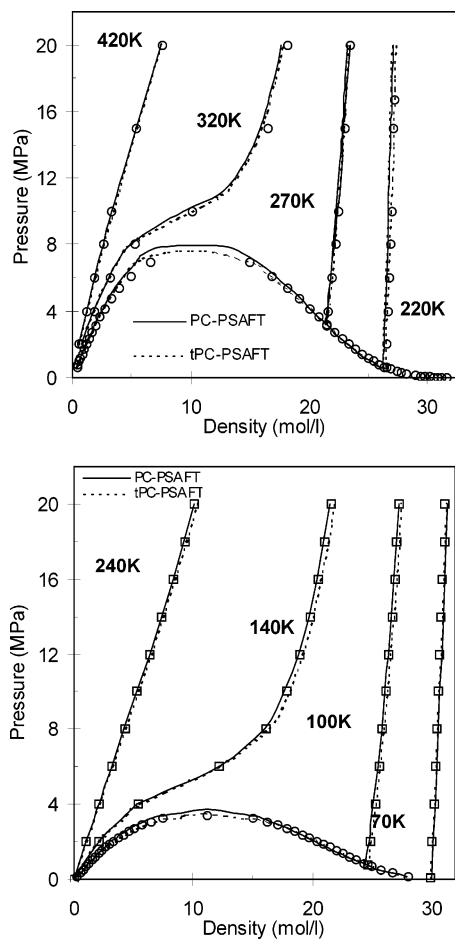


Figure 5. Experimental data (points) and EoS correlation (lines) for the saturation curve and the density at subcritical and supercritical conditions of carbon dioxide (top) and nitrogen (bottom).

In Figure 7 (top), experimental data and tPC-SAFT predictions are shown for water. Model predictions are in reasonably good agreement with experimental data, while deviations increase at lower temperatures. The second virial coefficient of nitrogen calculated on the basis of tPC-SAFT is shown in Figure 7 (bottom). Of course, the quadrupole moment of nitrogen is expected to have an effect only at subcritical temperatures ($T_c = 126.192$ K),⁵⁵ where the agreement is indeed very good.

Accurate calculation of caloric properties is important for a number of engineering applications. Inclusion of polar interactions is expected to improve significantly model predictions. It has been reported that SAFT and Peng–Robinson result in poor predictions of the liquid heat capacity of methanol and fluorinated hydrocarbons and that SWTEOS (square-well theoretical EoS) predictions deviate significantly (about 35%) from the experimental values of the isochoric heat capacity of compressed liquid carbon dioxide in the pressure range of 7–32 MPa.^{10,56} In this work, the isochoric heat capacity, C_v , of carbon dioxide and of nitrogen at 50 bar was calculated. The results are shown in Figure 8 and are in good agreement with the experimental data.^{57,58}

An additional important derivative property is the Joule–Thomson coefficient, μ_J . Here, μ_J of nitrogen, one of the most common low-temperature refrigerants,⁵⁹ was calculated at two different pressures. In Figure 9, experimental data⁵⁸ and tPC-SAFT predictions are shown. The model is very accurate in all cases, including prediction of the locus of (T, P) states in which $\mu_J = 0$, known as the Joule–Thomson inversion curve

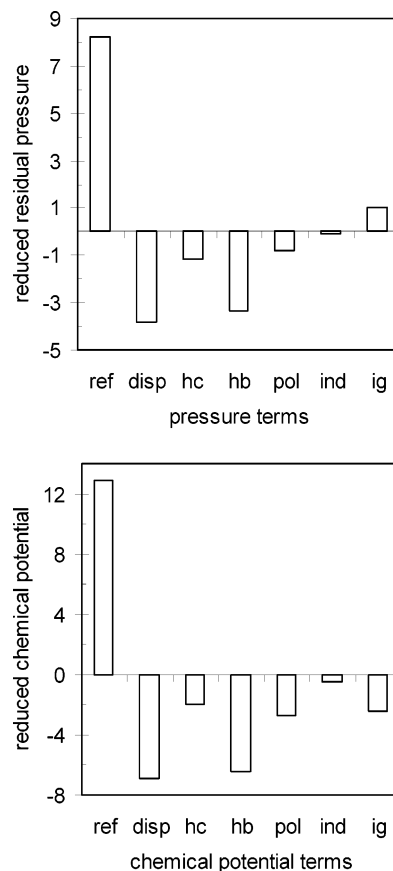


Figure 6. Contribution of the reference term (ref), the dispersion term (disp), the hard-chain term (hc), the hydrogen-bonding term (hb), the polar term (pol), the dipole–induced dipole term (ind), and the ideal gas term (ig) in pressure (top) and chemical potential (bottom) of saturated liquid water at 460 K from PC-SAFT.

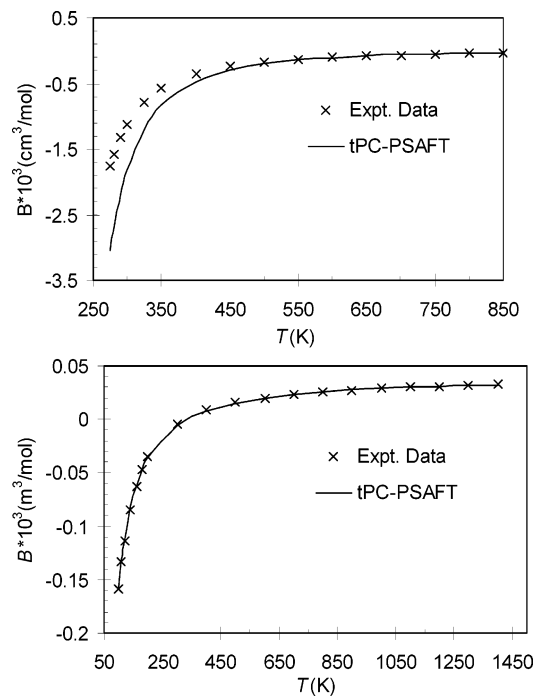


Figure 7. Experimental data⁴⁶ and tPC-SAFT predictions for the second virial coefficient of (top) water and (bottom) nitrogen.

(JTIC). JTIC is very important in low-temperature refrigeration.^{59,60} In Figure 10, prediction of the JTIC curve of carbon dioxide from tPC-SAFT is shown. Model predictions are in

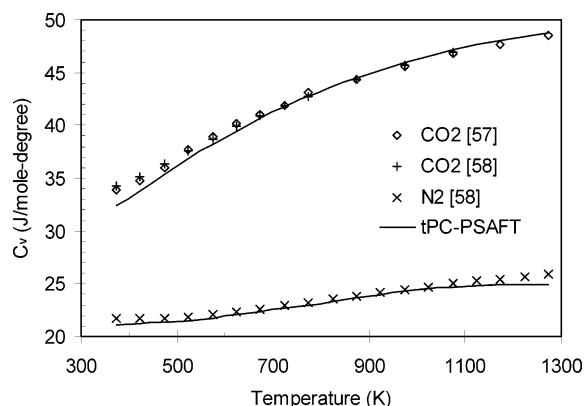


Figure 8. Experimental data^{57,58} and tPC-PSAFT predictions for the isochoric specific heat of carbon dioxide and nitrogen at 50 bar.

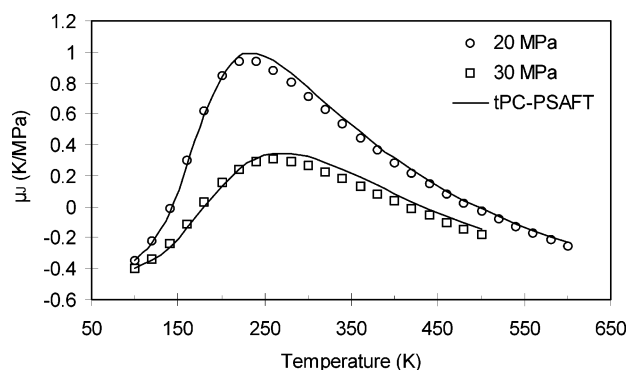


Figure 9. Experimental data⁵⁹ and tPC-PSAFT predictions for the Joule–Thomson coefficient of nitrogen at 20 and 30 MPa.

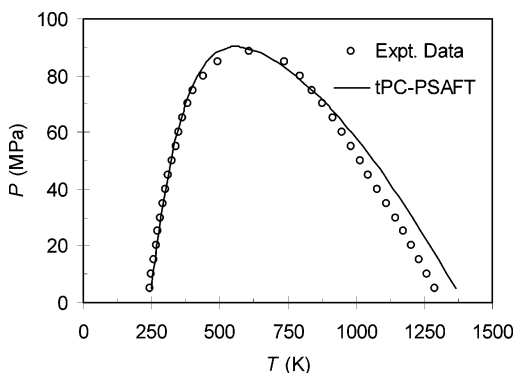


Figure 10. Experimental data⁵⁸ and tPC-PSAFT predictions for the Joule–Thomson inversion curve of carbon dioxide.

very good agreement with experimental data,⁵⁸ especially at low and medium temperatures where most carbon dioxide applications exist. Deviations observed above 900 K are in general smaller compared to deviations reported for other SAFT models.⁶⁰

Conclusions

The PC-SAFT model was extended to polar fluids based on a rigorous statistical mechanics model³. The new PC-PSAFT was used to model successfully the phase equilibria and other thermodynamic properties of various quadrupolar fluids. The model was shown to be accurate against molecular simulation results for quadrupolar fluids. A simplified version of the model was developed that is expected to be suitable for engineering calculations. The tPC-PSAFT is equally accurate as the PC-

PSAFT with the use of an additional pure component parameter. Currently, the model is extended to mixtures of fluids that exhibit various types of polar interactions.

References and Notes

- (1) Prausnitz, J. M.; Lichtenthaler, R. N.; Gomes de Azevedo, E. *Molecular Thermodynamics of Fluid-Phase Equilibria*, 3rd ed.; Prentice Hall: Englewood Cliffs, NJ, 1999.
- (2) Gray, C. G.; Gubbins, K. E. *Theory of Molecular Fluids*; Clarendon: Oxford, U.K., 1984; Vol. 1.
- (3) Larsen, B.; Rasaiah, J. C.; Stell, G. *Mol. Phys.* **1977**, *33*, 987.
- (4) Gubbins, K. E.; Twu, C. H. *Chem. Eng. Sci.* **1978**, *33*, 863.
- (5) Vimalchand, P.; Donohue, M. D. *Ind. Eng. Chem. Fundam.* **1985**, *24*, 246.
- (6) Saager, B.; Fischer, J. *Fluid Phase Equilib.* **1992**, *72*, 67.
- (7) Müller, A.; Winkelmann, J.; Fischer, J. *AIChE J.* **1996**, *42*, 1116.
- (8) Weingerl, U.; Wendland, M.; Fischer, J.; Müller, A.; Winkelmann, J. *AIChE J.* **2001**, *47*, 705.
- (9) Weingerl, U.; Fischer, J. *Fluid Phase Equilib.* **2002**, *202*, 49.
- (10) Benavides, A. L.; Guevara, Y.; Estrada-Alexanders, A. F. *J. Chem. Thermodyn.* **2000**, *32*, 945.
- (11) Benavides, A. L.; Guevara, Y. *J. Phys. Chem. B* **2003**, *107*, 9477.
- (12) Guevara, Y.; Benavides, A. L. *Mol. Phys.* **1996**, *89*, 1277.
- (13) Wertheim, M. S. *J. Stat. Phys.* **1984**, *35*, 19.
- (14) Wertheim, M. S. *J. Stat. Phys.* **1984**, *35*, 35.
- (15) Chapman, G. C.; Gubbins, K. E.; Jackson, G.; Radosz, M. *Ind. Eng. Chem. Res.* **1990**, *29*, 1709.
- (16) Huang, S. H.; Radosz, M. *Ind. Eng. Chem. Res.* **1990**, *29*, 2284.
- (17) Gross, J.; Sadowski, G. *Ind. Eng. Chem. Res.* **2001**, *40*, 1244.
- (18) Jog, P. K.; Chapman, W. G. *Mol. Phys.* **1999**, *97*, 307.
- (19) Jog, P.; Sauer, S.; Blaesig, J.; Chapman, W. G. *Ind. Eng. Chem. Res.* **2001**, *40*, 4641.
- (20) Sauer, S. G.; Chapman, W. G. *Ind. Eng. Chem. Res.* **2003**, *42*, 5687.
- (21) Chapman, W. G.; Sauer, S. G.; Ting, D.; Ghosh, A. *Fluid Phase Equilib.* **2004**, *217*, 137.
- (22) Tumakaka, F.; Sadowski, G. *Fluid Phase Equilib.* **2004**, *217*, 233.
- (23) Tumakaka, F.; Gross, J.; Sadowski, G. *Fluid Phase Equilib.* **2005**, *228–229*, 89.
- (24) Gross, J. *AIChE J.* **2005**, *51*, 2556.
- (25) Gross, J.; Vrabec, J. *AIChE J.* **2006**, *52*, 1194.
- (26) Karakatsani, E. K.; Spyriouni, T.; Economou, I. G. *AIChE J.* **2005**, *51*, 2328.
- (27) Rasaiah, J.; Stell, G. *Chem. Phys. Lett.* **1974**, *25*, 519.
- (28) Stell, G.; Rasaiah, J. C.; Narang, H. *Mol. Phys.* **1974**, *27*, 1393.
- (29) Laidler, K. J.; Meiser, J. H. *Physical Chemistry*, 2nd ed.; Houghton-Mifflin: Boston, MA, 1995.
- (30) Vega, C. *Mol. Phys.* **1992**, *75*, 427.
- (31) Vega, C.; Saager, B.; Fischer, J. *Mol. Phys.* **1989**, *68*, 1079.
- (32) Stogryn, D. E.; Stogryn, A. P. *Mol. Phys.* **1966**, *11*, 371.
- (33) Buckingham, A. D. *Chem. Br.* **1965**, *1*, 54.
- (34) Quinn, W. E.; Baker, J. M.; LaTourrette, J. T.; Ramsey, N. F. *Phys. Rev.* **1958**, *112*, 1929.
- (35) Gräff, G.; Runolfsson, O. *Z. Phys.* **1965**, *187*, 140.
- (36) Lide, R. D. *Handbook of Chemistry and Physics*, 75th ed.; CRC Press: Boca Raton, FL, 1994.
- (37) Topliss, R. J.; Dimitrelis, D.; Prausnitz, J. M. *Comput. Chem. Eng.* **1988**, *12*, 483.
- (38) Rushbrooke, G. S.; Stell, G.; Høye, J. S. *Mol. Phys.* **1973**, *26*, 1199.
- (39) Nezbeda, I. *Czech. J. Phys.* **1998**, *48*, 117.
- (40) Walsh, J. M.; Guedes, H. J. R.; Gubbins, K. E. *J. Phys. Chem.* **1992**, *96*, 10995.
- (41) Boulougouris, G. C.; Voutsas, E. C.; Economou, I. G.; Theodorou, D. N.; Tassios, D. P. *J. Phys. Chem. B* **2001**, *105*, 7792.
- (42) Kolafa, J.; Nezbeda, I. *Mol. Phys.* **2000**, *98*, 1505.
- (43) Kettler, M.; Nezbeda, I.; Chialvo, A. A.; Cummings, P. T. *J. Phys. Chem. B* **2002**, *106*, 7537.
- (44) Nezbeda, I.; Pavlíček, J. *Fluid Phase Equilib.* **1996**, *116*, 530.
- (45) Nezbeda, I.; Weingerl, U. *Mol. Phys.* **2001**, *99*, 1595.
- (46) Daubert, T. E.; Danner, R. P. *Physical and Thermodynamic Properties of Pure Compounds: Data Compilation*; Hemisphere: New York, **2001**.
- (47) Nezbeda, I.; Lísal, M. *Mol. Phys.* **2001**, *99*, 291.
- (48) Suresh, S. J.; Elliott, J. R., Jr. *Ind. Eng. Chem. Res.* **1992**, *31*, 2783.
- (49) Economou, I. G.; Tsonopoulos, C. *Chem. Eng. Sci.* **1997**, *52*, 511.
- (50) Yakoumis, I. V.; Kontogeorgis, G. M.; Voutsas, E. C.; Hendriks, E. M.; Tassios, D. P. *Ind. Eng. Chem. Res.* **1998**, *37*, 4175.
- (51) Jedlovsky, P.; Brodholt, J. P.; Bruni, F.; Ricci, M. A.; Soper, A. K.; Vallauri, R. *J. Chem. Phys.* **1998**, *108*, 8528.
- (52) Kalinichev, A. G.; Bass, J. D. *Chem. Phys. Lett.* **1994**, *231*, 301.
- (53) Luck, W. A. P. *Angew. Chem., Int. Ed. Engl.* **1980**, *19*, 28.

- (54) Gogonea, V.; Băleanu-Gogonea, C.; Osawa, E. *J. Mol. Struct. (THEOCHEM)* **1998**, 432, 177.
- (55) Tsonopoulos, C. *AIChE J.* **1974**, 20, 263.
- (56) Perez, V.; Chapman, W. *AIChE Spring Meeting Conference Proceedings* Houston, TX, March 19-23, 1995.
- (57) Price, D. *Chem. Eng. Data Ser.* **1956**, 1, 83.
- (58) *NIST Chemistry Webbook*; NIST Standard Reference Database 69; June 2005.
- (59) Bejan, A. *Advanced Engineering Thermodynamics*; John Wiley & Sons: New York, 1988.
- (60) Colina, C. M.; Turens, L. F.; Gubbins, K. E.; Olivera-Fuentes, C.; Vega, L. F. *Ind. Eng. Chem. Res.* **2002**, 41, 1069.